Research Square

Preprints are preliminary reports that have not undergone peer review.
They should not be considered conclusive, used to inform clinical practice,
or referenced by the media as validated information.

Satellite-Based Assessment of Forest-Cover Dynamics and Evidence of Mining Activities in Three Forest Reserves in Ghana (2016–2025)

Benjamin Sekum

bsekum@ug.edu.gh

University of Ghana

Research Article

Keywords: Forest-cover change, mining disturbance, Sentinel-2, stratified accuracy assessment, mining encroachment, forest reserves

Posted Date: November 24th, 2026

DOI: https://doi.org/10.21203/rs.3.rs-11777899/v1

License: This work is licensed under a Creative Commons Attribution 4.0 International License.
Read Full License

Additional Declarations: No competing interests reported.

Satellite-Based Assessment of Forest-Cover Dynamics and Evidence of Mining Activities in Three Forest Reserves in Ghana (2016–2025)

Benjamin Sekum

University of Ghana (Institute of Statistical, Social and Economic Research-ISSER), Accra, Ghana

bsekum@ug.edu.gh

https://orcid.org/0000-0002-9127-612X

Abstract

Forest protection in Ghana, intersects with the economic importance of resource extraction and forest-dependent livelihoods. Mining in recent years has and still threatens Ghana's forest reserves through

vegetation clearance, excavation and disturbance of river corridors. This study therefore examined forest-cover change and mining evidence in Upper Wassaw, Oda River and Apamprama during 2016–2025, combining Dynamic World land-cover maps, a Sentinel-2 mining screen and historical-image interpretation. Stratified estimates used 3,109 annual and 1,350 paired reference observations. Estimated net tree-cover losses were 1,001.65 ha, 812.31 ha and 1,057.23 ha, respectively. Apamprama's annual tree-cover stock declined by 28.63%, compared with 7.72% in Upper Wassaw and 4.97% in Oda River. Reference-adjusted mining areas in 2025 were 830.42 ha, 755.03 ha and 854.64 ha within the assessed reserve frames. Mining evidence overlapped 73.91%, 61.95% and 80.45% of estimated gross tree-cover loss. Screen omission rates of 36.26%, 19.40% and 51.64% demonstrated that mapped priority footprints understated mining extent. Qualitative image interpretation suggested progression from reserve fringes from 2016 towards interiors and workings aligned with Offin and Oda River channels in inspected locations in 2025. The gradual rapid encroachment of people into these forest reserves is alarming and concerning and hence requires strong and tighter protection and laws to ensure it is brought to a halt. Published evidence identified concerns involving water quality, mercury exposure and occupational hazards; these were implications rather than locally measured health outcomes.

Keywords:

Forest-cover change; mining disturbance; Sentinel-2; stratified accuracy assessment; mining encroachment; forest reserves

Introduction

Forests sustain biodiversity, regulate climate and water systems, and support livelihoods through food, fuel, timber and other ecosystem services (Shrestha et al., 2025; Upadhyay & Singh, 2024). Tropical forests alone support approximately 62% of the world's terrestrial vertebrate species, underscoring their conservation importance (Pillay et al., 2022). Globally, forests cover approximately 4.14 billion hectares, representing 32% of the land area (Food and Agriculture Organization of the United Nations [FAO], 2025). Despite slowing deforestation rates, continuing forest loss threatens these ecological and socioeconomic functions. Effective conservation therefore requires reliable information on where forest change occurs and which pressures shape it.

In Ghana, forest protection intersects with the economic importance of resource extraction and forest-dependent livelihoods. Hajjar (2015) reported that small and medium-scale forest enterprises supported income and livelihoods for approximately three million people, illustrating the sector's socioeconomic significance. Gold mining creates competing demands for land because vegetation clearance, excavation, access infrastructure and processing can transform forest and agricultural landscapes. Schueler et al. (2011) documented mining-related deforestation, farmland loss and agricultural displacement in western Ghana, demonstrating that extraction can generate pressures beyond the immediate mining footprint.

Satellite-based research further demonstrates the scale of mining-related landscape change. Barenblitt et al. (2021) estimated that approximately 47,000 hectares of vegetation in southwestern Ghana were converted to mining between 2005 and 2019, including encroachment within protected areas. At Oda River Forest Reserve, Abugre et al. (2025) reported a 5.9% reduction in forest cover between 2018 and 2023 alongside substantial expansion of mapped mining areas. More recently, Dong et al. (2025) documented extensive forest disturbance in Ghana's protected areas during 2023–2024, identifying Oda River among the affected reserves. These findings demonstrate that protected designation alone does not ensure forest retention.

Forest-reserve governance has also attracted national debate. Research in Atewa Range Forest Reserve identified regulatory weaknesses and institutional interference that undermine conservation (Mensah-Odum et al., 2025). The Environmental Protection (Mining in Forest Reserves) Regulations, 2022 (L.I. 2462), became a focus of advocacy over mining risks. Its revocation in December 2025 was welcomed by civil-society organisations, including A Rocha Ghana, which emphasised the continuing need for forest protection and restoration (Coalition Against Galamsey–Ghana et al., 2025). However, Barend, (2026) in examining the regulation found no evidence of widespread vegetation loss attributable to the policy change. Observed mining disturbance and the causal effects of legislation therefore require separate assessment.

Remote sensing provides a practical means of monitoring reserves repeatedly across space and time. Forkuor et al. (2020) demonstrated the value of Sentinel-1 time series for monitoring mining-related changes in southwestern Ghana while documenting limitations associated with observation conditions. Dong et al. (2025) further showed that combining Landsat, Sentinel-1 and Sentinel-2 observations can improve disturbance detection.

Building on previous research, this study provides a consistent comparison of land-cover change and mining disturbance in Upper Wassaw, Oda River and Apamprama forest reserves between 2016 and 2025. It connects benchmark land-cover maps, tree-cover transitions and evaluation of a mining screen within a common assessment framework. Consistent class definitions and sampling weights support meaningful comparisons despite differences in reserve size and land-cover composition. Reference observations both

inside and outside the mining screen allow reliability and omissions to be evaluated. This approach addresses the need to distinguish the mapped disturbance footprint from reference-based estimates of affected area and their uncertainty.

The study aims to characterize land-cover composition in 2016, 2020 and 2025; estimate tree-cover loss, gain, net change and conversion pathways; evaluate the 2025 mining screen against interpreted reference observations; and compare reserve-level estimates while accounting for classification and area uncertainty. It also examines the spatial association between tree-cover loss and mining evidence as well as its implication on the environment and economy. These objectives provide evidence on landscape conditions without claiming to establish mining legality, operational scale or the causal impact of legislation.

By combining reserve-level comparison with explicit assessment of uncertainty, the study can support forest surveillance, restoration planning and targeted field verification. Its findings are relevant to the Forestry Commission, environmental regulators and institutions responsible for managing mining pressures. More broadly, the analysis contributes evidence for forest governance, biodiversity conservation and Ghana's climate and sustainable-development commitments.

Materials and Methods

Study area and rationale for selecting the three reserves

Upper Wassaw, Oda River and Apamprama forest reserves were purposively selected as comparative case studies for examining forest-cover change and potential mining disturbance in Ghana's gold-mining landscapes. Their relevance rests on independently documented mining encroachment within designated forest reserves and the ecological implications of disturbance in these landscapes. Upper Wassaw provides a historically documented southwestern case: Barenblitt et al. (2021) identified it as having the largest mapped mining footprint among the 28 protected areas examined in their study. Oda River and Apamprama provide complementary cases within the Ashanti forest landscape, where the Forestry Commission has documented illegal mining in both reserves and highlighted their watershed functions and importance to downstream water users (Boateng, 2023). Recent satellite-based evidence of substantial forest disturbance in Oda River further demonstrates the relevance of sustained monitoring in this setting (Dong et al., 2025).

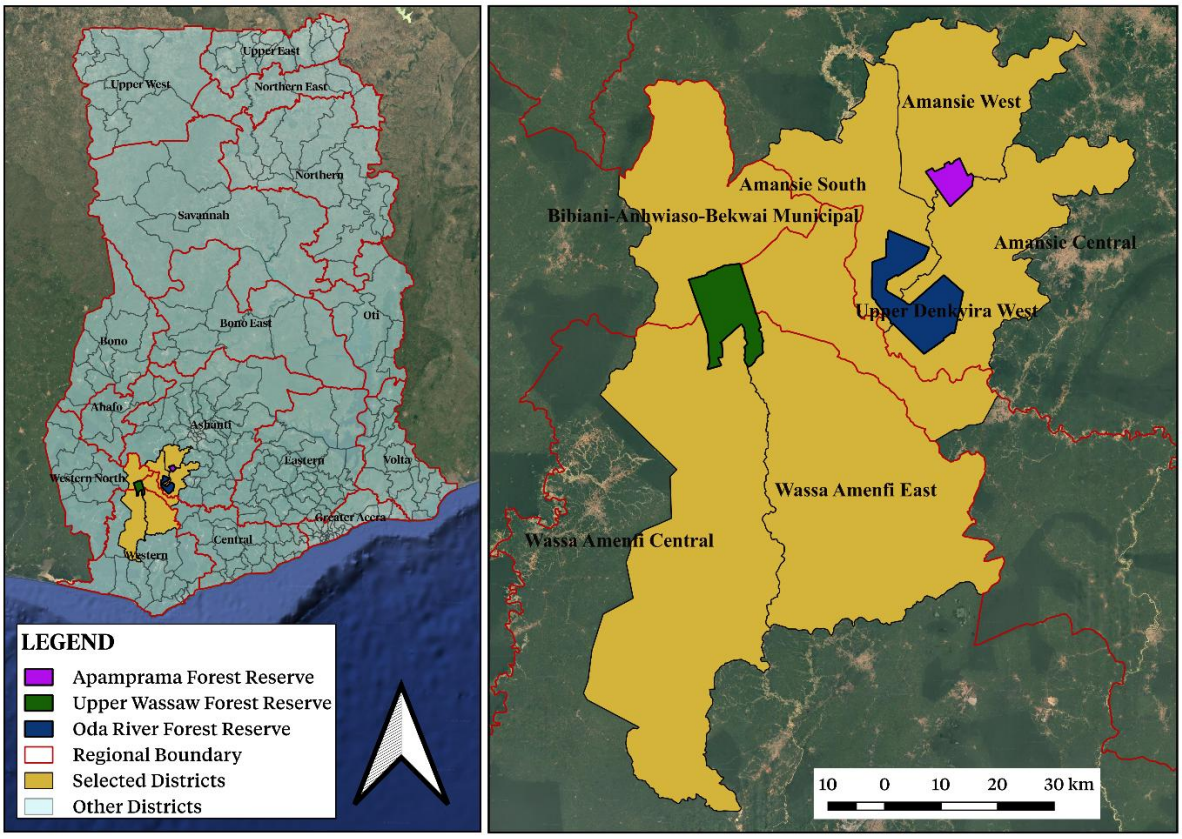


Figure 1A Geographical Map of the Forest Reserves

Source: Authors' construct.

Each reserve was analyzed within one boundary geometry applied to all benchmark years. The three reserves together provided a basis for comparing forest-change patterns across geographically distinct mining landscapes using common observation years, land-cover definitions and analytical procedures. Their differing extents also allow absolute area changes to be considered alongside proportional forest loss, providing context for assessing the relative magnitude and extent of disturbance. The comparison focuses on changes between 2016, 2020 and 2025 and the spatial distribution of mining evidence within the reserve boundaries. The selection supports detailed analysis of environmentally relevant cases; findings are therefore interpreted within these three reserves rather than extrapolated statistically to all forest reserves in Ghana.

Research design and analytical workflow

A retrospective comparative design combined quantitative remote sensing with qualitative image interpretation and a focused review of policy and health evidence. Spatial processing comprised boundary selection, annual satellite compositing, seven-class land-cover mapping, construction of tree-cover changes and mining-screen layers, stratified reference sampling and historical-image interpretation. The study adopted Google Earth Engine as the main processing tool (Gorelick et al., 2017).

The annual reference samples estimated land-cover stocks for 2016, 2020 and 2025. Paired reference samples estimated endpoint transitions and 2025 mining-screen performance. The original sample tables

listed the sampling groups, the number of pixels in each group, and the mapped land-cover classes. Sample IDs were used to match these records with the completed manual interpretations. Classification disagreements were retained, and the assessed maps were not retrained using the reference labels. The study also adopted a broader image review, qualitative observations on how encroachment starts from the boundaries and gradually creep into the main reserves comparing the three satellite images for the reference years (2016,2020,2025).

Satellite datasets and forest-reserve boundaries

Annual land-cover maps were produced using Dynamic World V1 (GOOGLE/DYNAMICWORLD/V1), which provides nine-class land-cover predictions derived from Sentinel-2 Level-1C imagery at a nominal spatial resolution of 10 m (Brown et al., 2022). The dataset allows predictions to be aggregated over user-defined periods, and its coverage from June 2015 made it possible to map the 2016 baseline. The annual maps were generated from these existing predictions without training a local classifier.

The 2016 image composite used top-of-atmosphere imagery from COPERNICUS/S2_HARMONIZED, while the 2020 and 2025 composites used surface-reflectance imagery from COPERNICUS/S2_SR_HARMONIZED. This difference was necessary because the Earth Engine surface-reflectance collection begins in March 2017 (Google Earth Engine, 2026b, 2026c). Mining screening used the 2025 surface-reflectance composite and did not involve comparisons of numerical thresholds across the two reflectance processing levels. Cloud probabilities were obtained from COPERNICUS/S2_CLOUD_PROBABILITY (Google Earth Engine, 2026d). The selected spectral bands comprised blue, green, red, near-infrared and two shortwave-infrared bands.

Forest-reserve boundaries were obtained from the World Database on Protected Areas (WDPA) polygon collection (WCMC/WDPA/current/polygons). The search was first restricted to Ghana, after which each of the three reserves was selected by its exact name. Ghana's outline was obtained from the United States Department of State's simplified Large Scale International Boundary dataset (USDOS/LSIB_SIMPLE/2017). Since WDPA is updated periodically, the boundary geometry used in the analysis is an important record for reproducing the study (UNEP-WCMC and IUCN, 2026). The same geometry was used for all years within each reserve. Before processing, all collections were checked to confirm that they contained data, ensuring that empty inputs were not mistaken for landscape conditions.

Image preprocessing, land-cover classes and annual map production

Satellite collections were filtered to the boundary of each reserve and to the period from 1 January of the target year to 1 January of the following year, excluding the latter date. Each map therefore summarised conditions across a full year rather than representing a single image date. Annual Dynamic World maps were produced by assigning each pixel its most frequent label during the year. The input product already included the provider's cloud and shadow masking (Google Earth Engine, 2026a).

For the supporting Sentinel-2 composites, images were matched to their cloud-probability assets using their system identifiers. Images without a matching asset were excluded, and pixels with a cloud probability of 40% or more were masked. Additional edge masks were applied using bands B8A and B9. For the 2016 top-of-atmosphere imagery, pixels flagged as opaque cloud or cirrus in QA60 were also excluded. For surface-reflectance imagery, scene-classification values 0, 1, 3, 8, 9, 10 and 11 were excluded. The selected

reflectance bands were divided by 10,000, and the remaining observations were combined into annual median composites.

The original Dynamic World classes were grouped into seven study classes. Trees were assigned to forest/tree cover; grass and shrub/scrub were combined as shrub/grassland; crops became cropland; built area became built-up; and bare ground became bare/disturbed land. Water and flooded vegetation retained their original meanings, while snow/ice was excluded from the valid study classes. All maps used a 10 m grid in WGS84/UTM zone 30N (EPSG:32630), with the affine transform [10, 0, 0, 0, 10, 0].

The tree-cover class served as the operational measure of forest, although it does not distinguish natural forest from plantations or other woody cover. Built-up and bare/disturbed land similarly describe surface conditions and do not, on their own, establish the presence of mining. The blue, green, red and near-infrared bands have a native resolution of 10 m, whereas the selected shortwave-infrared bands have a resolution of 20 m. Resampling these coarser bands to the common 10 m grid standardised the analysis units without adding spatial detail to the original observations.

Land-cover area estimation and transition analysis

The analysis retained both mapped and reference-adjusted area estimates. Mapped areas described the extent of the classified cells, while reference-adjusted estimates used the interpreted sample labels to estimate land-cover areas within the sampling frame. This frame consisted of full 10 m cells whose centres fell within a reserve and met the relevant data-validity criteria. Each eligible cell represented 0.01 ha, ensuring that the population counts used for weighting corresponded to the cells available for sampling.

For each stratum h, the expansion weight was calculated as:

$$w_h = \frac{N_h}{n_h},$$

where N_h is the number of eligible cells in the stratum and n_h is the actual number sampled. The estimated area of reference class k was:

$$\hat{A}_k = 0.01 \sum_h N_h \, \hat{p}_{hk},$$

where $\hat{p}_{hk}$ is the observed proportion of sampled cells in stratum h interpreted as class k. This weighting accounted for the different sampling fractions assigned to common and rare mapped classes (Olofsson et al., 2013).

Transitions between 2016 and 2025 were estimated from the paired reference sample using an indicator for each combination of starting and ending classes. The resulting seven-by-seven table showed persistence along the diagonal and conversion between classes elsewhere. Forest-conversion pathways were summarised by the 2025 destination class among locations interpreted as tree cover in 2016. These estimates describe differences between the two endpoints; they do not resolve any additional clearing, cultivation or recovery that may have occurred between them.

Population counts were taken from the original sampling-design exports and retained even when reference labels differed from the mapped strata. The frequencies of interpreted labels were not substituted for these counts, thereby preserving the selection probabilities and weights of the original grid-based design.

Forest-cover loss, gain, net change and change rates

Tree-cover loss occurred where a location interpreted as class 1 in 2016 belonged to another class in 2025. Gain described the reverse transition, while stable tree cover referred to locations in class 1 at both endpoints. Stable non-tree cover included all locations outside class 1 in both years, including those that changed between non-tree classes. Gross loss and gain were estimated separately from the paired reference indicators. Net loss was calculated as gross loss minus gross gain, with positive values indicating a decline in tree cover.

Tree-cover stocks were also estimated separately for each benchmark year. Differences between these annual estimates were reported as stock changes and distinguished from net change calculated from the paired sample, since the valid-data masks could differ between years. The common frame shared by the paired observations provided the principal estimates of gross loss, gain and net change for 2016–2025. Any difference between a stock change and paired net change was therefore examined in relation to the sampling frames before being treated as a calculation error.

Proportional stock decline was calculated as the difference between starting and ending tree-cover area, divided by starting area and multiplied by 100. Mean annual stock change was the signed difference between ending and starting area divided by the elapsed number of years. Compound annual change was calculated as:

$$r = 100\left[\left(\frac{A_{\text{end}}}{A_{\text{start}}}\right)^{1/t} - 1\right],$$

where A_{start} and A_{end} are the starting and ending tree-cover areas, and \(t\) is the elapsed period: four years for 2016–2020, five years for 2020–2025 and nine years for 2016–2025. These rates summarise changes between benchmark stocks rather than year-by-year clearing histories.

Potential mining-disturbance screening and reference verification

Potential mining disturbance was screened by combining mapped land-cover conversion with four spectral indices calculated from the 2025 surface-reflectance composite:

$$\text{NDVI} = \frac{\text{NIR} - \text{red}}{\text{NIR} + \text{red}},$$

$$\text{MNDWI} = \frac{\text{green} - \text{SWIR1}}{\text{green} + \text{SWIR1}},$$

$$\text{NDTI} = \frac{\text{red} - \text{green}}{\text{red} + \text{green}},$$

$$\text{BSI} = \frac{(\text{SWIR1} + \text{red}) - (\text{NIR} + \text{blue})}{(\text{SWIR1} + \text{red}) + (\text{NIR} + \text{blue})}.$$

NIR and SWIR1 refer to the near-infrared and first shortwave-infrared bands, respectively. NDTI was used as a spectral indicator and was not converted into a measured sediment concentration.

Four conditions were assessed: NDVI below 0.40, BSI above zero, MNDWI above 0.10 and NDTI above zero. Each condition contributed one point when satisfied, giving an evidence score from zero to four.

Locations were assigned higher priority for potential mining where they had mapped tree cover in 2016, built-up, bare/disturbed or water cover in 2025, and an evidence score of at least two. A supplementary water/pit flag identified locations with tree cover in 2016, water in 2025, and both the water and turbidity-related conditions satisfied. The rules were assessed as specified, without adjusting thresholds to improve agreement with the completed reference labels.

Using historical high-resolution imagery in Google Earth Pro, the reference interpreter recorded whether mining evidence was present or absent in 2025. Bare ground or water alone was insufficient to classify a location as mining. Final codes were checked against their descriptions and interpretation notes. The assessment identified visible mining evidence; it did not establish licensing status, legality, extraction method or the operating scale of every site. Confirmation of mining also did not, by itself, validate the supplementary water/pit flag.

Reference mining labels were available only for 2025. They supported estimation of mining evidence at that endpoint, including locations outside the priority screen. Earlier historical imagery informed the qualitative description of encroachment but did not provide independently validated mining-area estimates for 2016 or 2020. Tree-cover changes were therefore not treated as a numerical record of mining expansion, and the adjusted 2025 mining area was not used to calculate a historical mining-growth rate.

Reference sampling and accuracy assessment

Annual reference samples were selected through stratified random sampling, with a target of 50 observations per mapped land-cover class in each year. Where a class contained fewer than 50 eligible cells, all cells were sampled. The final annual dataset contained 3,109 observations: 1,050 from Upper Wassaw, 1,033 from Oda River and 1,026 from Apamprama. The 2020 shrub/grassland stratum in Oda River and the 2016 built-up stratum in Apamprama were fully enumerated.

The paired sample used six mutually exclusive strata: stable tree cover; tree-cover loss flagged by the priority screen, excluding flagged water/pits; loss with flagged water/pits; other loss, including locations with unavailable spectral evidence; tree-cover gain; and non-tree cover at both endpoints. Where flags overlapped, the water/pit category took precedence. Sampling 75 locations from each stratum produced 450 paired observations per reserve. The inclusion of unflagged locations allowed the assessment to identify mining evidence missed by the screen.

The base random seed was 20261023. The target year was added for annual sampling, while 100 was added for paired sampling. Fixed sample identifiers, coordinates and 10 m cell outlines supported interpretation and matching. The original sampling strata were retained when reference labels disagreed with mapped classes. Quality checks confirmed that identifiers were unique, class codes were valid, and mining codes agreed with their descriptions. No unresolved mining category remained after these checks.

Weighted confusion matrices were used to estimate overall, user's and producer's accuracy. Commission and omission errors were calculated as the complements of user's and producer's accuracy, respectively. For the mining screen, user's accuracy represented precision and producer's accuracy represented recall. Indicator-based stratified estimators allowed for the fact that the paired sampling strata differed from the binary mining classes (Stehman, 2014). All reference labels were assigned by one interpreter. The assessment did not include a second-interpreter reliability study or field measurements of water chemistry or health outcomes.

Area uncertainty and screening sensitivity

Sampling uncertainty was estimated for the specified probability design and eligible grid frame, treating the reference labels as fixed. For an indicator total, the stratified variance estimator was:

$$\widehat{\mathrm{Var}}(\hat{T}) = \sum_h N_h^2 \left(1 - \frac{n_h}{N_h}\right) \frac{s_h^2}{n_h},$$

where s_h^2 is the within-stratum sample variance of the indicator. Standard errors for ratios were estimated using Taylor linearisation. Fully enumerated strata contributed no sampling variance. However, a sample containing no errors or no observations of a class can also produce a zero plug-in variance, even though errors or class occurrences may remain among unsampled cells.

To address this limitation, the principal 95% confidence bounds were obtained by inverting exact hypergeometric population-count tails within each stratum. Bonferroni allocation across the component counts protected the coverage of each reported parameter, and the resulting bounds were propagated to area estimates, accuracy ratios and net change. These conservative bounds applied to individual parameters; they did not form a single simultaneous 95% region covering every result in the manuscript. The procedure supplemented the general area-estimation framework of Olofsson et al. (2014).

Mining-screen sensitivity was assessed using producer's accuracy, omission error and the difference between mapped screening area and reference-adjusted mining area. The retained thresholds defined the screen evaluated against the reference observations. Precision used the known mapped-positive strata, while the other accuracy ratios used their corresponding estimated domain totals. Omission error was the estimated false-negative total divided by the estimated reference-positive total. Commission error was the estimated false-positive total divided by the mapped-positive total. These calculations used expanded population estimates rather than unweighted percentages from the deliberately balanced stratified sample.

Locations with unavailable screening flags were retained in the common endpoint frame and distinguished from locations with observed negative flags. Screening accuracy was estimated within the domain where flags were known, while mining area was estimated across the full common land-cover frame.

The confidence bounds quantify sampling variability. They do not capture every source of uncertainty associated with image interpretation, temporal alignment, land-cover definitions or boundary geometry. High observed agreement was therefore reported alongside confidence bounds and class-specific results, with these remaining sources of uncertainty acknowledged.

Cross-reserve synthesis, policy interpretation and reproducibility

Results were compared across reserves using consistent benchmark years, class definitions, grids and weighting procedures. Areas in hectares described the scale of tree-cover loss and mining, while proportions expressed pressure relative to initial tree cover or the eligible sampling frame. The overlap between mining and tree-cover loss was estimated from joint reference indicators and interpreted as a spatial association. The analysis did not use a causal model to attribute all tree-cover loss to mining.

Historical-image interpretation described apparent movement from reserve fringes towards the interior and river-aligned workings at inspected locations. These observations were considered separately from the sample-based area estimates. The analysis did not calculate edge-distance bands, penetration depths, river-

buffer proportions or fragmentation indices. References to the Offin River and Oda River described the interpreted landscape and did not imply that either river crossed every reserve. Comparisons with earlier studies accounted for their boundaries, observation periods and land-cover definitions, distinguishing similarities in spatial patterns from agreement in estimated areas.

The documentary review examined original Ghanaian studies on forest condition, encroachment and catchment impacts, alongside relevant regulations and health guidance. Study dates, spatial coverage and measured outcomes were checked before comparisons were made. Policy interpretation considered the 2022 regulations, the 2025 amendment and reports of revocation in late 2025. The discussion of health implications drew on WHO guidance and independent research on Ghanaian rivers. This focused review provided context for the findings; it did not constitute a meta-analysis, causal policy evaluation or local exposure assessment.

Statistical analysis was carried out using Python 3.12.14, NumPy 2.3.5, SciPy 1.17.0 and Stata. Original samples, sampling-design tables, reviewed reference labels, scripts and audit results were retained, and outputs were compiled in Excel. Final maps were further processed, designed and exported in QGIS. The Earth Engine processing version FIX20261028B recorded the datasets, annual filters, cloud-masking rules, thresholds, random seeds and grid parameters. Quantitative findings remained linked to the original assessed maps, with qualitative observations and literature-based interpretations identified separately.

Results

Data coverage, map accuracy and assessment uncertainty

All 4,459 reference records were linked to their corresponding entries in the sampling-design tables. These comprised 3,109 annual observations and 1,350 paired observations. Most annual samples contained 350 observations. The exceptions were Oda River in 2020 and Apamprama in 2016, which contained 333 and 326 observations, respectively, because smaller strata were fully enumerated(Table 1). The common sampling frames for the endpoint analysis covered 13,600.05 ha in Upper Wassaw, 16,817.00 ha in Oda River and 3,707.48 ha in Apamprama. Screening flags were unavailable for 11 population cells in Upper Wassaw and 12 in Oda River, although flags were available for all sampled locations.

Annual weighted overall accuracy ranged from 99.914% to 100% (Table 1). There were 14 disagreements, all involving shrub/grassland and cropland in 2016. Despite this high overall agreement, accuracy was lower for some individual classes. For example, producers' accuracy for cropland in Oda River was 63.11% in 2016. The paired change assessment showed complete agreement in the observed sample, although the conservative lower accuracy bounds were approximately 92.95%. These results supported the interpretation of the estimated changes, with the confidence bounds accounting for sampling uncertainty.

Table 1. Annual land-cover accuracy with conservative individual 95% bounds.

Reserve	Year	Sample n	Errors	Weighted OA (%)	95% bounds (%)
Upper Wassaw	2016	350	8	99.914	89.202 to 99.986
Upper Wassaw	2020	350	0	100.000	89.344 to 100.000

Upper Wassaw	2025	350	0	100.000	89.344 to 100.000
Oda River	2016	350	6	99.996	89.337 to 99.999
Oda River	2020	333	0	100.000	89.344 to 100.000
Oda River	2025	350	0	100.000	89.344 to 100.000
Apamprama	2016	326	0	100.000	89.349 to 100.000
Apamprama	2020	350	0	100.000	89.348 to 100.000
Apamprama	2025	350	0	100.000	89.348 to 100.000

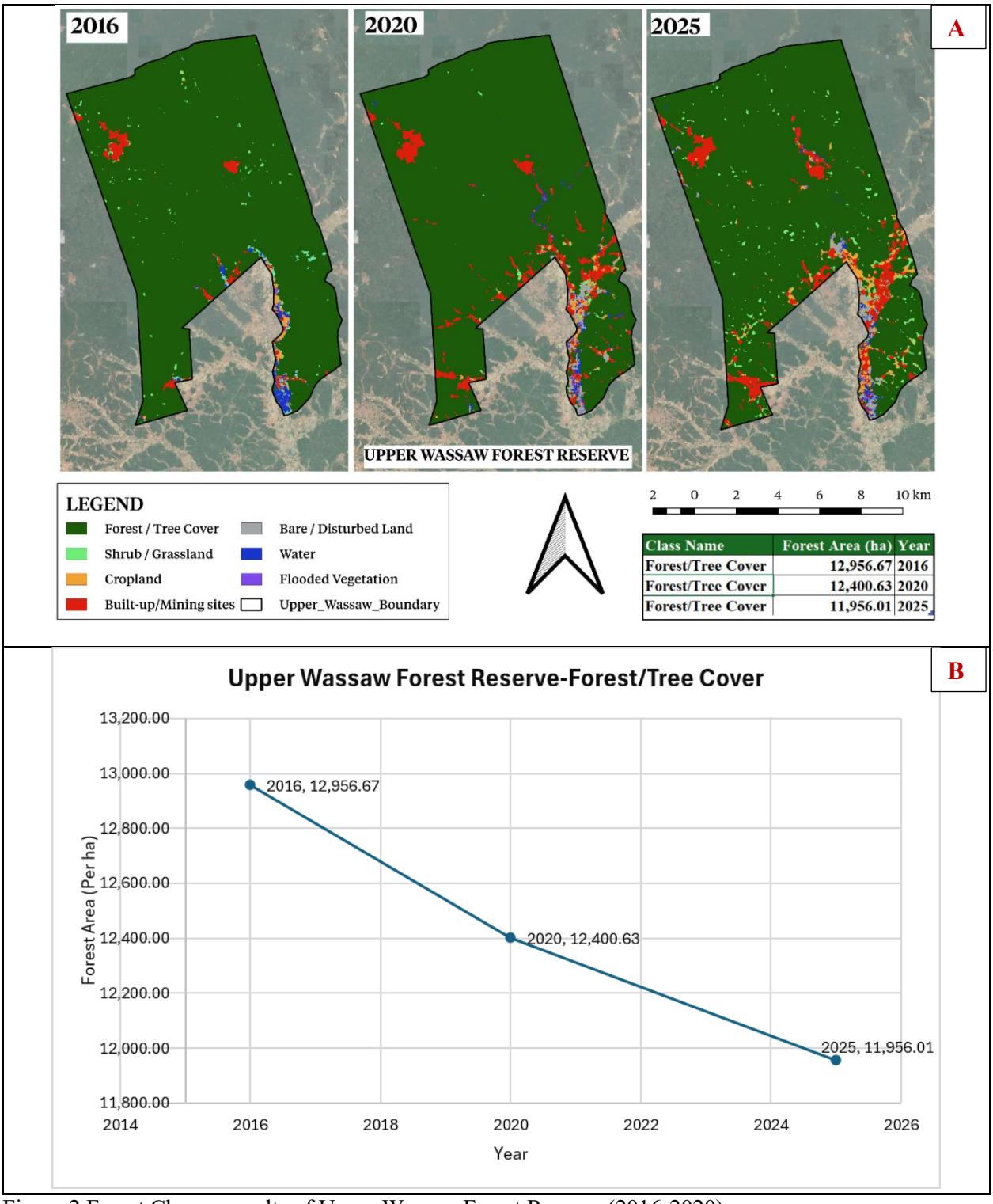
Source: Authors' calculations. OA = overall accuracy.

Land-cover composition and spatial patterns in 2016, 2020 and 2025

Upper Wassaw Forest Reserve

Tree cover remained dominant in all reserves, but the balance between forest and non-tree classes changed markedly. Upper Wassaw declined from 12,956.67 ha of tree cover in 2016 to 12,400.63 ha in 2020 and 11,956.01 ha in 2025 (Fig.1). Tree-cover shares were approximately 95.27%, 91.17% and 87.90%. Built-up cover/mining sites increased from 255.55 to 831.21 ha between the first and final benchmarks; cropland increased from 80.77 to 312.91 ha and shrub/grassland from 65.87 to 236.42 ha. All these results indicate a rapid growing degradation of the Upper wassaw forest reserve with a ripple impact on biodiversity and the environment at large.

The mapped net forest loss was lower in 2020–2025 (444.71 ha) than in 2016–2020 (557.59 ha), as gross loss declined slightly, and forest gain increased from 167.96 to 261.44 ha. The reference-adjusted comparison of the 2016 and 2025 endpoints estimated 1,123.60 ha of gross forest loss and 121.95 ha of gain, yielding a net loss of 1,001.65 ha.



381 Figure 2 Forest Change results of Upper Wassaw Forest Reserve (2016-2020)

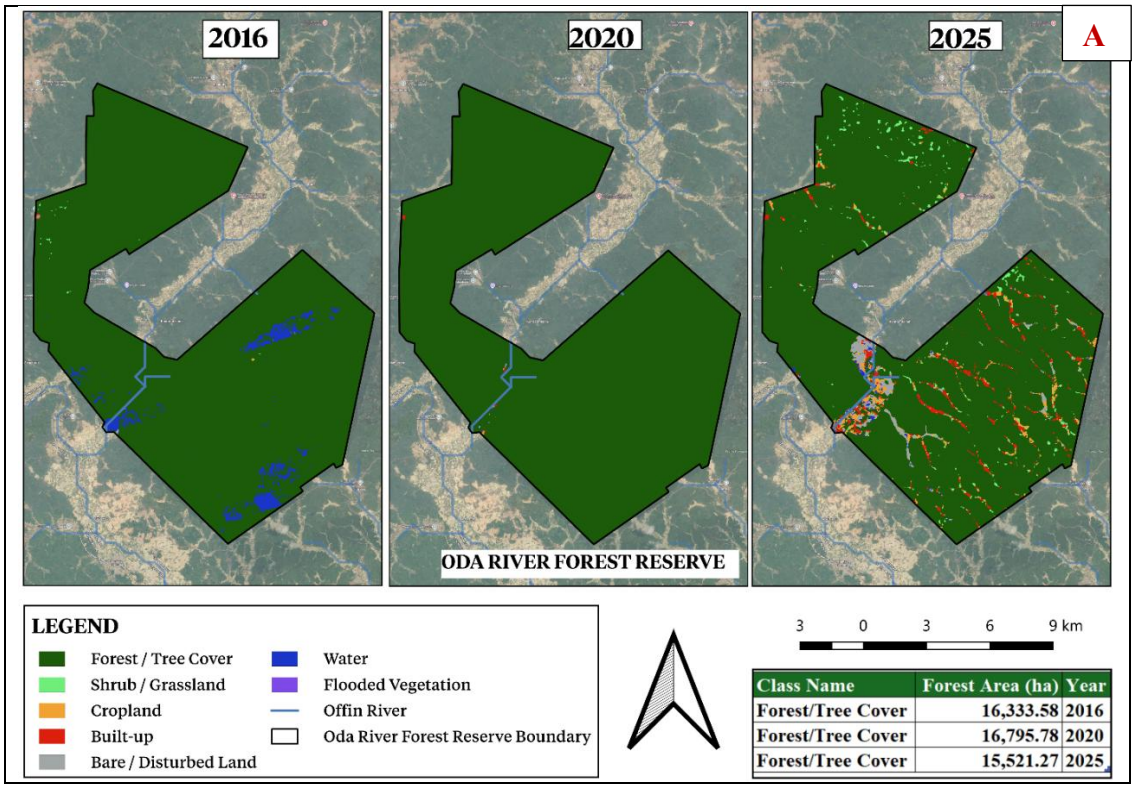
382 Source: Authors' construct

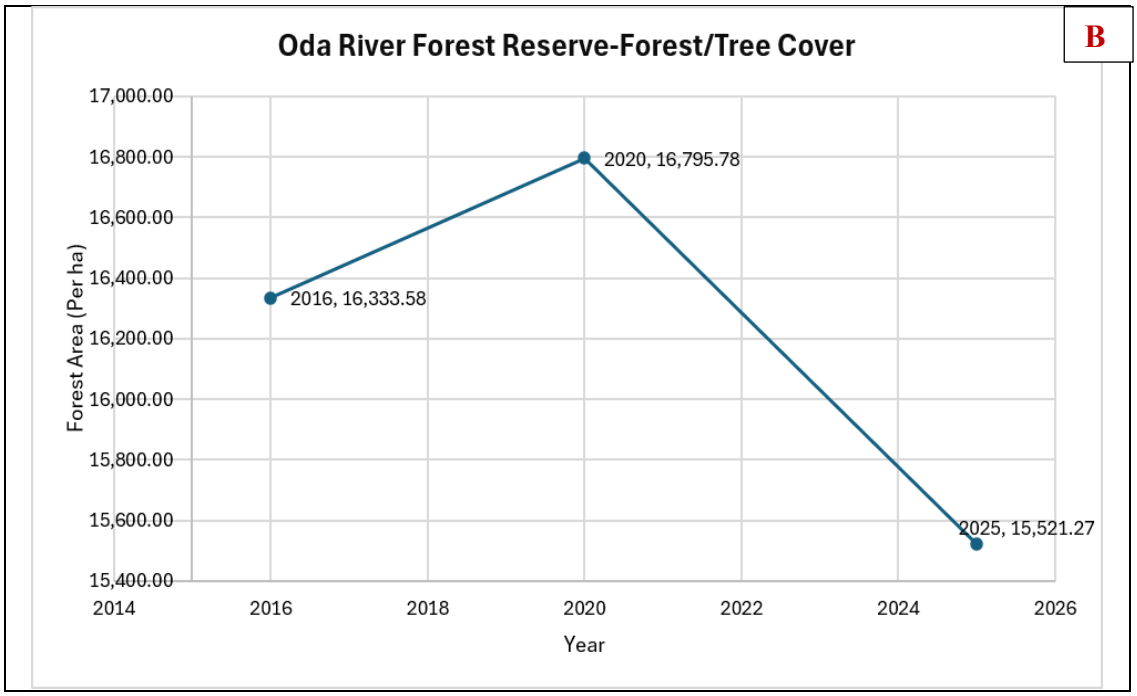
383

384 Oda River Forest Reserve

Tree cover remained the dominant land-cover class in Oda River Forest Reserve. Its estimated extent rose from 16,333.58 ha (97.13%) in 2016 to 16,795.78 ha (99.85%) in 2020, before falling to 15,521.27 ha (92.28%) in 2025(Fig. 2). Between 2016 and 2025, built-up cover/mining sites increased from 2.66 to 403.20 ha, cropland from 1.61 to 309.99 ha, and bare or disturbed land from 6.60 to 277.43 ha. The 2025 map shows bare and disturbed land concentrated near the Offin River crossing, with patches of cropland, shrub and grassland, and built-up cover scattered across the southeastern part of the reserve.

The maps show a net forest gain of 462.12 ha in 2016–2020, followed by a net loss of 1,275.14 ha in 2020–2025. In the second interval, gross forest loss reached 1,279.65 ha and forest gain fell to 4.50 ha. The reference-adjusted comparison of the 2016 and 2025 endpoints estimated 1,218.84 ha of gross forest loss and 406.53 ha of gain, yielding a net loss of 812.31 ha.





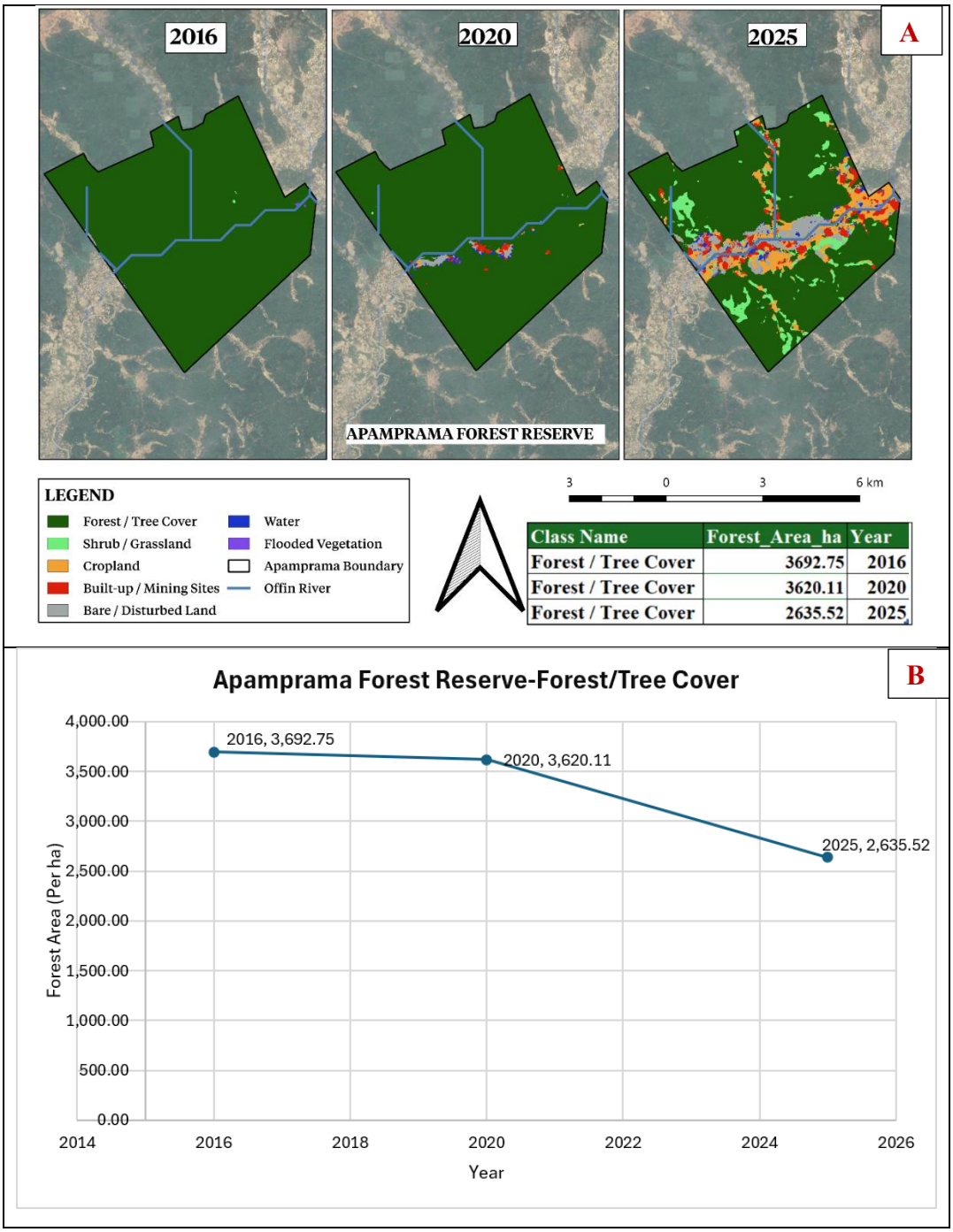
395 Figure 3 Forest Change results of Oda River Forest Reserve (2016-2020)

396 Source: Authors' construct

397

398 Apamprama Forest Reserve

399 Reference-adjusted tree cover declined from 3,692.75 ha (99.60%) in 2016 to 3,620.11 ha (97.64%) in 2020
400 and 2,635.52 ha (71.09%) in 2025(Fig. 3). Between 2016 and 2025, cropland expanded from 0.57 to 364.33
401 ha, shrub and grassland from 1.01 to 251.85 ha, and bare or disturbed land from 7.42 to 226.50 ha. In 2020,
402 the map shows small patches of non-forest cover along the Offin River. By 2025, non-forest cover occupied
403 a wider band along the river through the reserve, particularly towards the eastern boundary.



404 Figure 4 Forest Change results of Apramprama Forest Reserve (2016-2020)

405 Source: Authors' construct

406

407 Forest-cover extent, loss, gain and net change

408 Across the three forest reserves, estimated tree cover declined from 32,983.00 ha in 2016 to 32,816.52 ha
409 in 2020 and 30,112.80 ha in 2025. The total decrease was 2,870.20 ha, equivalent to 8.70% of the combined

2016 tree-cover estimate. Tree cover remained the dominant land-cover class in all three reserves, but its trajectory varied by reserve (Fig. 4).

In Upper Wassaw, estimated tree cover declined at each successive benchmark, from 95.27% in 2016 to 91.17% in 2020 and 87.90% in 2025. Oda River's tree-cover share increased from 97.13% to 99.85% between 2016 and 2020, before declining to 92.28% in 2025. Apamprama showed the largest decline in tree-cover share. It decreased from 99.60% in 2016 to 97.64% in 2020 and 71.09% in 2025.

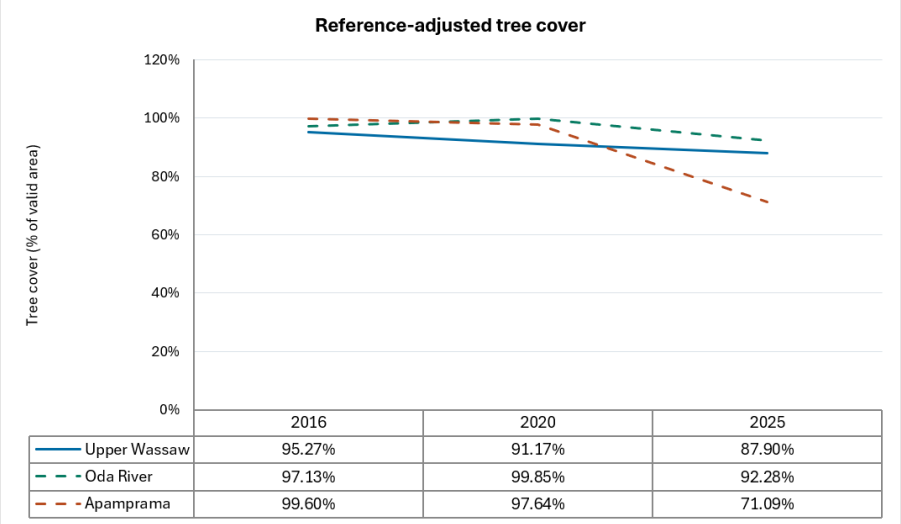


Figure 5: Reference-adjusted tree cover in Upper Wassaw, Oda River and Apamprama, 2016–2025.
Source: Authors' construct. NB:Tree cover is expressed as a percentage of the area with valid observations in each reserve and year.

The combined decrease in estimated tree-cover area was 166.48 ha in 2016–2020 and 2,703.72 ha in 2020–2025 (Table 2A). Oda River shifted from an increase of 462.20 ha in the first interval to a decrease of 1,274.51 ha in the second, the largest decline after 2020. Over the same intervals, Apamprama's mean annual decline increased from 18.16 to 196.92 ha per year, while Upper Wassaw's slowed from 139.01 to 88.92 ha per year.

Relative to the 2016 estimates, tree-cover area declined by 7.72% in Upper Wassaw, 4.97% in Oda River and 28.63% in Apamprama by 2025. Over nine elapsed years, these changes corresponded to compound annual rates of −0.89%, −0.57% and −3.68%, respectively.

Table 2A. Change in estimated annual tree-cover area by reserve and year pair (ha).

Reserve	2016–2020	2020–2025	2016–2025
Upper Wassaw	−556.04	−444.62	−1,000.66
Oda River	+462.20	−1,274.51	−812.31
Apamprama	−72.64	−984.59	−1,057.23
Three reserves combined	−166.48	−2,703.72	−2,870.20

Source: Authors' calculations

On the area with valid observations at both the 2016 and 2025 endpoints, the paired reference assessment estimated 3,404.79 ha of gross tree-cover loss and 533.60 ha of gross gain across the three reserves, giving a net loss of 2,871.19 ha (Table 2B). Oda River had the greatest gross loss (1,218.84 ha) and the greatest gain (406.53 ha), resulting in the smallest estimated net loss (812.31 ha). Apamprama had the largest estimated net loss (1,057.23 ha), with only 5.12 ha of estimated gain. Its conservative 95% bounds for net loss, 680.99 to 1,266.51 ha, were the only ones that excluded zero.

In Upper Wassaw, the paired net loss of 1,001.65 ha was 0.99 ha greater than the decline obtained by comparing the annual area estimates. The difference reflects the slightly different sets of valid cells used in the two analyses.

Table 2B. Reference-adjusted tree-cover loss, gain and net loss on the common 2016–2025 analysis area.

Reserve	Stable tree cover (ha)	Gross loss (ha)	Gross gain (ha)	Net loss (ha)	Conservative 95% bounds for net loss (ha)
Upper Wassaw	11,832.83	1,123.60	121.95	1,001.65	−151.90 to 1,997.04
Oda River	15,114.74	1,218.84	406.53	812.31	−580.49 to 2,076.87
Apamprama	2,630.40	1,062.35	5.12	1,057.23	680.99 to 1,266.51
Three reserves combined	**29,577.97**	**3,404.79**	**533.60**	**2,871.19**	—

Source: Authors' calculations

3.4 Major land-cover transitions and forest-conversion pathways

Reference-based transitions varied among reserves (Table 4). In Upper Wassaw, built-up cover was the largest estimated destination of tree-cover loss (597.76 ha; 53.20%), followed by cropland (229.79 ha) and shrub/grassland (174.33 ha). Oda River showed a more evenly distributed pattern, led by bare/disturbed land (345.03 ha; 28.31%), followed by built-up cover (299.84 ha), cropland (284.80 ha) and shrub/grassland (260.39 ha). In Apamprama, cropland dominated (354.83 ha; 33.40%), followed by shrub/grassland (259.63 ha) and bare/disturbed land (255.37 ha).

Uncertainty bounds were wide, including 451.90–1,617.56 ha for Upper Wassaw's tree-cover-to-built-up transition and 252.89–668.03 ha for Apamprama's tree-cover-to-cropland transition. Rankings therefore describe point estimates rather than established statistical differences. These weighted estimates describe endpoint cover without resolving intermediate land-use changes or demonstrating direct mining causation. Mining evidence was assessed separately and could not be inferred by combining built-up, bare/disturbed and water transitions.

Table 3: Reference-adjusted destinations of 2016 tree cover by 2025 hectares.

Reserve	Shrub/ grass	Cropland	Built-up	Bare/ disturbed	Water	Flooded vegetation
Upper Wassaw	174.33	229.79	597.76	75.32	46.41	0.00
Oda River	260.39	284.80	299.84	345.03	28.78	0.00
Apamprama	259.63	354.83	158.97	255.37	24.90	8.65

Source: Authors' calculations

Extent and spatial distribution of potential mining disturbance

Mapped priority-screen areas were 529.31 ha in Upper Wassaw, 608.56 ha in Oda River and 413.27 ha in Apamprama. All 150 sampled mapped-positive locations per reserve were confirmed as mining evidence. The screen nevertheless missed 38, 18 and 51 mining-positive observations, respectively, all in the other-loss stratum. Mining therefore extended beyond the footprint selected by the retained screening rule.

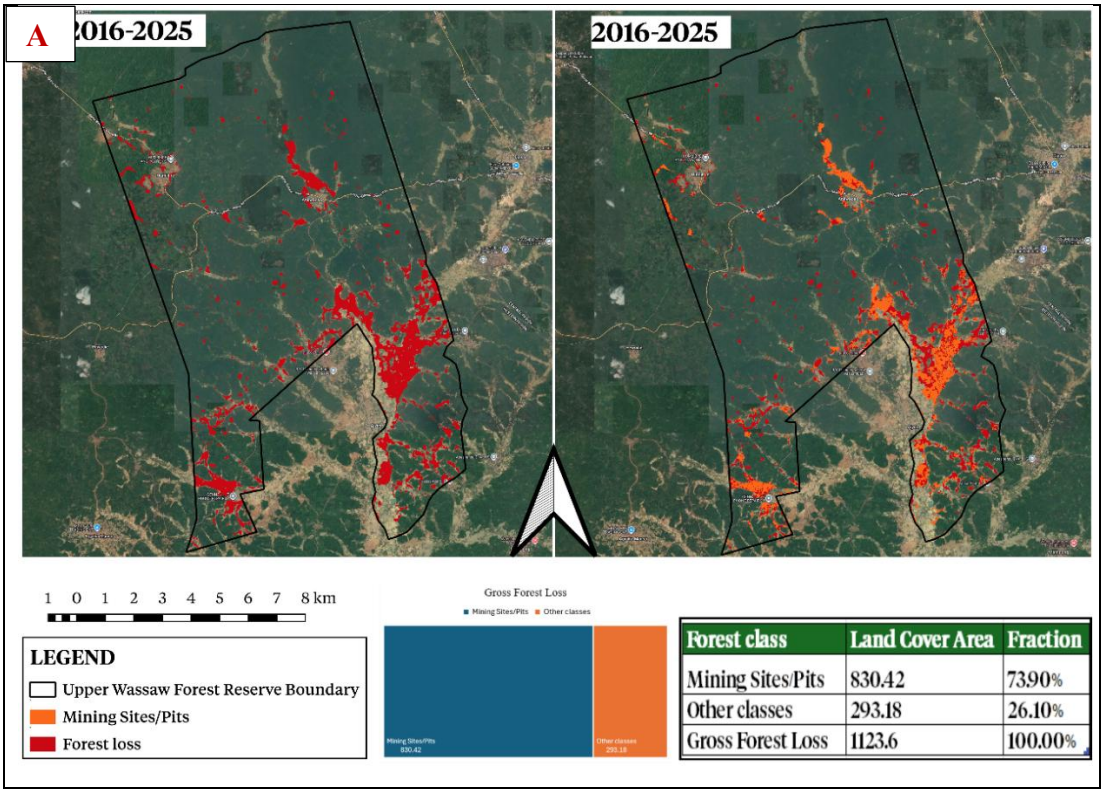
Weighted recall was 63.74% in Upper Wassaw, 80.60% in Oda River and 48.36% in Apamprama, with corresponding omission estimates of 36.26%, 19.40% and 51.64%. Recall bounds were 27.90–71.69%, 29.72–88.92% and 34.99–54.91%. Precision was 100% in each sample, with lower bounds near 94.33%.

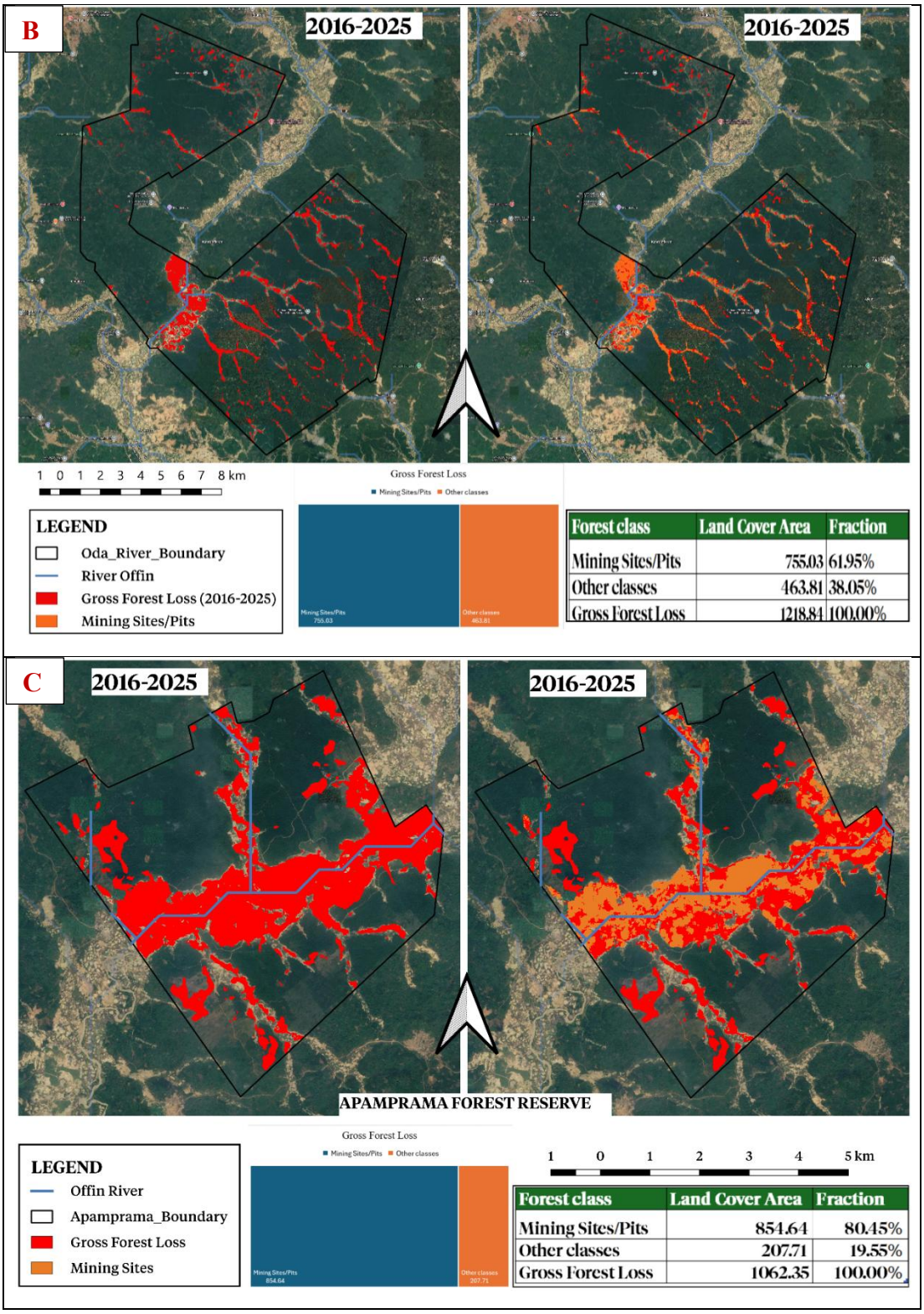
Table 4: Mapped mining priority area, reference-adjusted mining area and screen sensitivity.

Reserve	Mapped (ha)	Adjusted (ha)	Area 95% bounds (ha)	Recall (%)	Omission (%)
Upper Wassaw	529.31	830.42	701.10 to 1,801.07	63.74	36.26
Oda River	608.56	755.03	641.58 to 1,946.45	80.60	19.40
Apamprama	413.27	854.64	723.61 to 1,127.01	48.36	51.64

Source: Authors' calculations. Precision was 100% in the sample in each reserve, with lower 95% bonds of about 94.33%.

Reference-adjusted mining areas were 830.42 ha, 755.03 ha and 854.64 ha (Fig. 5). Their 95% intervals were 701.10–1,801.07 ha, 641.58–1,946.45 ha and 723.61–1,127.01 ha. These represented approximately 6.11%, 4.49% and 23.05% of the common frames. Additional area beyond the screen was 301.11, 146.47 and 441.37 ha.





472 Figure 6 Mining Evidence in the three Forest Reserves

473 Source: Authors' construct

Mining evidence overlapped 73.91%, 61.95% and 80.45% of estimated gross tree-cover loss. The respective overlap-fraction bounds were 32.68–90.78%, 25.77–85.17% and 55.97–90.91%. The interpreter also reported workings aligned with Offin and Oda River channels in the inspected landscape. No hydrological overlay or river-buffer share was calculated. This qualitative observation did not measure contaminant concentrations or demonstrate the timing and cause of every overlapping forest-loss event.

The adjustment exceeded mapped screening area by approximately 56.89% in Upper Wassaw, 24.07% in Oda River and 106.80% in Apamprama. These percentages compare two estimates of the 2025 footprint, and they do not measure expansion since 2016. The validated endpoint therefore establishes the importance of omitted mining while leaving earlier mining extents to further historical assessment.

Discussion

Galamsey pressure and the changing condition of forest reserves

The findings identify substantial forest change alongside a mining footprint larger than the priority screen suggests. Apamprama experienced the greatest proportional tree-cover stock decline and the highest reference-adjusted mining share, despite being the smallest reserve. Its 5.12 ha of estimated gain provided little offset to 1,062.35 ha of gross loss. Oda River combined greater gross loss with greater gain, while Upper Wassaw showed persistent stock decline. These differences demonstrate why retained forest percentage and net change alone provide an incomplete account of reserve condition.

The Oda River findings agree in direction with Abugre et al. (2025), who reported 5.9% forest decline during 2018–2023 and mining expansion from 52.78 to 1,059.85 ha, fastest during 2022–2023. The present 2016–2025 annual-stock decline was 4.97%, and adjusted 2025 mining area was 755.03 ha. These magnitudes are not interchangeable: the earlier study used forest/mining classes and a different mapped total, whereas this analysis retained seven cover classes and probability-based reference adjustment. The smaller 2025 mining estimate cannot establish a decline from the published 2023 value.

Upper Wassaw likewise has a well-documented but method-dependent mining history. Barenblitt et al. (2021) reported 466.29 ha within WDPA boundaries, whereas Gallwey et al. (2020) estimated approximately 1,300 ha of mining-related deforestation in winter 2018–2019 using Forestry Commission boundaries. Their estimate of more than 800 ha newly affected after 2015 belongs to the latter study. The present 830.42 ha estimate confirms substantial mining evidence within its own frame but does not resolve the differences between those inventories. Boundary harmonisation and matched definitions are necessary before interpreting their numerical ordering as temporal change (Table 6).

Apamprama extends the earlier account of boundary pressure in Snapir et al. (2017): reference-confirmed mining now contributes an estimated 23.05% of the analysed frame. This establishes present disturbance within the frame, without proving that every work originated at the boundary described earlier. Mining evidence overlapped 80.45% of estimated gross tree-cover loss there, compared with 73.91% in Upper Wassaw and 61.95% in Oda River. These are spatial associations rather than complete causal allocations of forest loss.

Alternative pathways remain material. Agricultural expansion accounted for 78% of forest loss in the Ashanti reserve landscapes studied during 1986–2015 by Acheampong et al. (2019). Wanyama et al. (2023) found that much reserve disturbance involved degradation from closed to open forest. These results support

retaining separate land-cover transitions and mining attributes. Plot evidence of vegetation absence in heavily mined Oda River sites further shows why ecological consequences can exceed what categorical area estimates describe (Abugre et al., 2025).

The confidence bounds affect how these comparisons should be expressed. Apamprama's conservative net-loss interval excluded zero under this construction, whereas the Upper Wassaw and Oda River intervals included it. This does not imply that no clearing occurred in the latter reserves: gross loss and gain are separate processes, and uncertainty around their difference is wider. Between-reserve rankings should likewise describe point estimates because the intervals overlap. Published studies supply corroboration of mining pressure, but do not remove the sampling uncertainty of the present estimates.

The three benchmark maps also leave timing unresolved within each interval. A location mapped as forest in 2016 and non-forest in 2025 could have experienced logging, cultivation and extraction in succession. Conversely, mining on previously cleared land need not produce new forest loss. This explains why mining area and forest-conversion areas should be retained as related but distinct outcomes. It also prevents a claim that all detected mining began after the regulation or after the 2020 benchmark.

Table 5: Published reserve evidence and interpretation of the current estimates.

Reserve	**Earlier evidence**	**Comparison with this study**
Upper Wassaw	Landsat: 466.29 ha within WDPA boundaries (Barenblitt et al., 2021). Sentinel-2: about 1,300 ha of mining-related deforestation in winter 2018–2019 using Forestry Commission boundaries (Gallwey et al., 2020).	Adjusted 2025 mining area: 830.42 ha. Differing boundaries and definitions prevent interpreting the numerical ordering as a measured decline or increase.
Oda River	Abugre et al. (2025): 5.9% forest decline during 2018–2023, with 1,059.85 ha of mining in 2023, from a forest/mining classification.	Annual-stock decline during 2016–2025: 4.97%; adjusted 2025 mining: 755.03 ha. Different endpoints, classes and reference adjustment prevent constructing one mining trend.
Apamprama	Snapir et al. (2017): boundary-adjacent mining ribbons in the 2011–2015 mapping; no equivalent 2025 inventory.	Adjusted 2025 mining: 854.64 ha, or 23.05% of the frame. Stock decline: 28.63%. These estimates extend reserve-specific evidence without quantifying movement from the earlier workings.

Source: Authors' compilation of the cited studies.

From reserve fringes towards forest interiors

The qualitative image interpretation suggests a gradual extension of mining activities from 2016 towards the reserve interior. This pattern is consistent with Tsai et al. (2019), who found reduced forest cover near reserve boundaries, and with the peripheral conversion reported for the Birim Basin by Nyamekye et al. (2021). The latter study also found comparatively little disturbance within reserve interiors during its earlier

observation window. Together, the studies identify edges as vulnerable locations while showing that substantial interior invasion is not an inevitable condition at every place or date. This provides a basis for concern about fragmentation and declining habitat quality beyond the excavated surface (Harper et al. (2005).

River-aligned disturbance and downstream implications

The indication or the reported mining activities along the Offin and Oda River channels, raises and its implication on the river bodies raises serious concerns. Hausermann et al. (2018) documented extensive mining-mediated transformation along a section of the Offin, including redirected waterways and abandoned water-filled pits. Their mixed-method evidence supported interpreting river-associated mining as a change to land and water systems, rather than solely as a loss of canopy. The present observations concern inspected locations and do not imply that both named rivers traverse all three reserves.

Evidence from elsewhere in Ghana reinforces the spatial interpretation. Adams and Hayakawa (2025) found that at least 49.7% of mapped mining area annually lay within 100 m of river channels in the Atewa landscape during 2018–2023. That percentage is not an estimate for Upper Wassaw, Oda River or Apamprama. Its relevance lies in demonstrating a measurable association between alluvial mining and channel proximity, which the present qualitative observations suggest should be tested locally. The same study's differing reserve-interior and surrounding-landscape trends also cautions against substituting basin-wide change for reserve-specific change.

Nunoo et al. (2022) provide direct water-quality evidence from the Offin, Oda and Pra rivers and nearby boreholes. Their analyses identified pollution and treatment concerns, strengthening the environmental rationale for protecting riparian vegetation and limiting sediment delivery from disturbed ground. These independently collected samples concern different locations and dates from the present reference observations. Their concentrations cannot be assigned to the mapped workings or used to diagnose current exposure around the reserves.

Removal of channel-side vegetation and excavation can expose sediment and alter drainage, providing plausible mechanisms for downstream effects. Satellite water discolouration and turbidity-related indices help locate areas requiring investigation, but do not identify individual chemicals or establish drinking-water safety. Catchment monitoring should therefore combine verified channel networks and mining locations with water and sediment sampling upstream and downstream of workings.

Forest-mining regulations and changes during the study period

The policy interpretation requires a distinction between permitting regulated extraction and legitimising unlicensed galamsey. Hilson and Nyame (2006) documented the forest-mining debate following exploration concessions awarded in 2001. Mining access therefore cannot be dated entirely to L.I. 2462. The 2022 instrument established environmental-management provisions and restricted mining in specified sensitive areas. Its original regulation 3(2) nevertheless provided for written presidential approval of mining in globally significant biodiversity areas in the national interest, subject to article 268 of the Constitution (Republic of Ghana, 2022). This exception is relevant to concerns about protection within reserves.

L.I. 2501 removed regulation 3(2) in 2025. The ministry's August statement subsequently sought revocation of both instruments, and Ghana News Agency reported revocation effective on 10 December 2025 (Republic of Ghana, 2025; Ministry of Environment, Science and Technology, 2025; Appiah-Osei, 2025). A Rocha Ghana and partner organisations (2023) had criticised the original framework for weakening

safeguards. Those concerns help explain the policy debate; they are not measurements of its ecological effects in these reserves.

The observed trajectories do not identify one uniform regulatory response. Annualised stock decline increased markedly after 2020 in Oda River and Apamprama but decreased in Upper Wassaw. Abugre et al.'s (2025) account of rapid Oda mining expansion during 2022–2023 adds temporal context without isolating the instrument's contribution. Dong et al. (2025) reported 18.5% ±4.7% forest disturbance in Oda River during 2023–2024, a substantially different measure from the present net stock change. That discrepancy warrants matched-boundary and disturbance-definition checks rather than treating the published percentage as numerical confirmation.

Governance mechanisms also extend beyond statutory wording. Botchwey and Crawford (2025) attribute the failure of the 2017–2024 national campaign partly to political involvement and protection within illicit mining networks. Their analysis identifies potential implementation problems, not proven explanations for individual clearings here. Evaluating policy effects requires dated permits, enforcement records, annual disturbance events and a defensible comparison design. Because 2020–2025 includes pre-regulation and post-regulation years, and the final annual composite scarcely extends beyond the reported repeal, this study supplies policy-relevant evidence rather than a causal policy estimate (Table 7).

Table 6: Regulatory chronology in relation to observation periods.

Period	Regulatory context	Interpretation for this study
2016 and 2020	Benchmark years preceding L.I. 2462	Provide earlier forest-stock observations; mining pressure may predate the instrument.
2022	L.I. 2462 provides a forest-mining framework, including the original regulation 3(2) exception	Occurs within the 2020–2025 interval, not at its beginning.
2025 amendment	L.I. 2501 removes regulation 3(2); August ministry request seeks wider revocation	The final observation year contains multiple regulatory stages.
December 2025	Revocation reported effective on 10 December by Ghana News Agency	The annual 2025 composite provides no sustained post-revocation comparison.

Sources: Republic of Ghana (2022, 2025); Ministry of Environment, Science and Technology (2025); Appiah-Osei (2025). This chronology is policy context, not a causal effect estimate.

Environmental health concerns and populations at risk

The health implications follow exposure pathways that extend beyond reserve boundaries. Where mercury is used for gold recovery, amalgam burning can expose workers and nearby residents to vapour. Environmental transformation and accumulation in aquatic food provide another potential route. WHO (2024) identifies neurological and kidney effects, with particular concern for fetal and early childhood

development. These mechanisms justify attention to workers, pregnant women, children and households using downstream resources, while local exposure requires direct assessment.

WHO (2016) also identifies dust, unsafe equipment, physical injury and stagnant-water hazards in artisanal mining settings. Silica-containing ore dust can contribute to serious respiratory disease, and suitable abandoned pits can provide vector habitat. The independent river analyses by Nunoo et al. (2022) support concerns about treatment requirements and household water supplies. Health effects therefore depend on substances, exposure routes and working conditions, not simply on the presence of a mine polygon or visibly muddy water.

The present study collected no clinical observations, exposure biomarkers, fish-contamination data or disease counts. Health concerns are consequently implications supported by external evidence rather than demonstrated outcomes among reserve-adjacent communities. Appropriate follow-up would link environmental measurements with occupational histories, drinking-water and food-use practices, and public-health assessment. This would distinguish populations with plausible exposure from those merely living near a mapped disturbance and support prevention proportionate to actual conditions (Table 8).

Table 7: Literature-based health pathways and evidence required locally.

Exposure pathway	**Potential concern**	**Evidence needed locally**
Mercury vapour where amalgam is burned	Neurological and kidney harm (WHO, 2024)	Processing history and appropriate air/exposure assessment
Contaminated aquatic food	Methylmercury developmental risk (WHO, 2024)	Fish sampling and dietary exposure assessment
Silica-containing ore dust	Serious respiratory disease (WHO, 2016)	Ore/dust characterisation and occupational assessment
Unsafe equipment or workings	Physical injury (WHO, 2016)	Incident records and site-safety inspection
Suitable stagnant-water conditions	Potential vector habitat (WHO, 2016)	Local vector ecology and disease surveillance
Impaired river-water quality	Water-treatment and household-supply concerns (Nunoo et al., 2022)	Current chemical and microbial water testing

Source: Authors' compilation of the cited studies. These are potential pathways identified from the literature. The present study measured no pollutant exposure, clinical outcome or disease prevalence.

Implications for forest protection monitoring and restoration

The practical priority is to connect forest surveillance with verification of mining beyond the visible priority footprint. Sample precision was high, but omission was substantial, especially in Apamprama. A narrow screen can support inspection priorities while still understating affected areas. The reference-adjusted estimates therefore complement the maps; they do not redraw each omitted activity. Sentinel-1 time series could complement future optical monitoring under persistent tropical cloud cover (Forkuor et al., 2020).

Monitoring should distinguish newly cleared forest, persistent workings and recovery, while examining reserve fringes and suspected routes into the interior. Annual categorical maps should also be complemented by canopy-condition measures where degradation may precede complete loss, as demonstrated in Ghanaian reserve research (Wimberly et al., 2022; Wanyama et al., 2023). River-corridor assessment requires verified hydrographic connections rather than assigning the same catchment interpretation to every reserve.

Restoration should address disturbed soils, drainage and riparian continuity alongside vegetation establishment. Apamprama's limited estimated gain indicates that recovery at the endpoint scarcely offset clearing; it does not establish the effectiveness of any restoration programme. Field assessment should determine whether tree-cover returns correspond to native vegetation, stable substrates and recovering ecological functions. Enforcement and restoration should be linked to community water security and livelihood conditions because the consequences extend across reserve and catchment boundaries.

An immediate extension would assemble dated image panels for the same peripheral, interior and river-adjacent locations. A consistent reserve outline, acquisition date and labelled channel would make the visual account reviewable. Subsequent mapping could estimate change within inward boundary bands and outward river buffers, while field inspections record actual land use and permit status. Environmental sampling should use catchment connections to select upstream and downstream locations, with public-health teams determining appropriate exposure assessment. These steps would turn the spatial interpretation into testable evidence and help distinguish persistent mining, new entry, abandoned workings and genuine vegetation recovery. They would also support evaluation of enforcement at the locations where disturbance is observed, rather than relying on aggregate reserve totals alone.

Conclusion

Upper Wassaw, Oda River and Apamprama experienced substantial forest-cover change within landscapes affected by galamsey during 2016–2025. Paired net tree-cover losses were 1,001.65, 812.31 and 1,057.23 ha, respectively, while reference-adjusted 2025 mining areas were 830.42, 755.03 and 854.64 ha. Apamprama combined the greatest proportional stock decline with the largest estimated mining share and the highest screen omission. These findings demonstrate the importance of assessing forest conditions and mining evidence together while retaining uncertainty.

Qualitative image interpretation suggested expansion from reserve fringe towards interiors and workings aligned with Offin and Oda channels in inspected locations. Relevant Ghanaian studies support concern about boundary pressure, river-associated disturbance and ecological degradation, although their numerical estimates are not interchangeable with this assessment. Mining–loss overlap indicates spatial association rather than exclusive attribution of every clearing to galamsey.

L.I. 2462 and its subsequent amendment and reported revocation provide a governance context, but the benchmark years cannot isolate regulatory effects. Water-quality deterioration, mercury exposure and occupational hazards are literature-supported concerns requiring local investigation. Forest protection should combine monitoring beyond priority screens with verified river-corridor assessment, enforcement and ecological restoration. Dated spatial analysis, environmental sampling and exposure assessment would establish the evidence needed to evaluate ecological and community-health consequences.

Statements and declarations

Funding Declaration

No funding was received for this study or for the preparation of this manuscript.

Competing interests

The author declares no competing interests.

Data availability

The satellite datasets and boundary layers used in this study are available through the Google Earth Engine Data Catalog under the identifiers listed in Materials and Methods. Historical imagery used for reference interpretation was accessed through Google Earth Pro. The sampling design files, interpreted reference labels, validation tables, and area estimates are available from the corresponding author on reasonable request.

Code availability

The Google Earth Engine scripts used for land-cover mapping and mining screening and the Python scripts used for accuracy assessment and area estimation are available from the corresponding author on reasonable request.

Author contributions

Benjamin Sekum designed the study, developed the analytical workflow, analysed the satellite imagery, interpreted the historical reference imagery, performed the statistical analysis, prepared the figures and tables, and drafted and revised the manuscript.

Ethics approval

Not applicable. The study used satellite data and historical imagery.

Consent to participate

Not applicable.

Consent to publish

Not applicable.

References

A Rocha Ghana and partner organisations. (2023). Mining in forest reserves: It is time to break through the silence. Press statement, 9 June 2023. https://ghana.arocha.org/wp-content/uploads/sites/15/2023/06/June-2023-L2462-state-of-FRs-2.pdf

Abugre, S., Asigbaase, M., Kumi, S., Nkoah, G., & Asare, A. (2025). Forest landscape degradation, carbon loss and ecological consequences of illegal gold mining in Ghana. Discover Forests, 1, 20. https://doi.org/10.1007/s44415-025-00020-5

Acheampong, E. O., MacGregor, C. J., Sloan, S., & Sayer, J. (2019). Deforestation is driven by agricultural expansion in Ghana's forest reserves. Scientific African, 5, e00146. https://doi.org/10.1016/j.sciaf.2019.e00146

Adams, L. B., & Hayakawa, Y. S. (2025). Mapping alluvial mine dynamics in the Atewa landscape in Ghana using Geographic Object-Based Image Analysis (GEOBIA) and GIS. Environmental Monitoring and Assessment, 197, 473. https://doi.org/10.1007/s10661-025-13892-z

Appiah-Osei, E. (2025). Ghana revokes controversial mining law, paving way for forest conservation. Ghana News Agency, 19 December 2025. https://gna.org.gh/2025/12/ghana-revokes-controversial-mining-law-paving-way-for-forest-conservation/

Barenblitt, A., Payton, A., Lagomasino, D., Fatoyinbo, L., Asare, K., Aidoo, K., Pigott, H., Som, C. K., Smeets, L., Seidu, O., & Wood, D. (2021). The large footprint of small-scale artisanal gold mining in Ghana. Science of the Total Environment, 781, 146644. https://doi.org/10.1016/j.scitotenv.2021.146644

Botchwey, G., & Crawford, G. (2025). Small-scale mining, environmental destruction and democracy capture: The Government of Ghana's failed "war on galamsey". Democratization, 32(8), 2091–2112. https://doi.org/10.1080/13510347.2025.2489018

Brown, C. F., Brumby, S. P., Guzder-Williams, B., Birch, T., Hyde, S. B., Mazzariello, J., Czerwinski, W., Pasquarella, V. J., Haertel, R., Ilyushchenko, S., Schwehr, K., Weisse, M., Stolle, F., Hanson, C., Guinan, O., Moore, R., & Tait, A. M. (2022). Dynamic World, Near real-time global 10 m land use land cover mapping. Scientific Data, 9, 251. https://doi.org/10.1038/s41597-022-01307-4

Dong, L., Tang, X., Mensah, F., Abubakari, B. A., Bratley, K. H., Olofsson, P., & Woodcock, C. E. (2025). Near real-time monitoring reveals extensive recent forest disturbance in Ghana's protected areas. Science of Remote Sensing, 12, 100299. https://doi.org/10.1016/j.srs.2025.100299

Forkuor, G., Ullmann, T., & Griesbeck, M. (2020). Mapping and monitoring small-scale mining activities in Ghana using Sentinel-1 time series (2015–2019). Remote Sensing, 12(6), 911. https://doi.org/10.3390/rs12060911

Gallwey, J., Robiati, C., Coggan, J., Vogt, D., & Eyre, M. (2020). A Sentinel-2 based multispectral convolutional neural network for detecting artisanal small-scale mining in Ghana: Applying deep learning to shallow mining. Remote Sensing of Environment, 248, 111970. https://doi.org/10.1016/j.rse.2020.111970

Google Earth Engine. (2026a). Dynamic World V1. Earth Engine Data Catalog. Accessed 2 November 2026. https://developers.google.com/earth-engine/datasets/catalog/GOOGLE_DYNAMICWORLD_V1

Google Earth Engine. (2026b). Harmonized Sentinel-2 MSI Level-1C top-of-atmosphere reflectance. Earth Engine Data Catalog. Accessed 2 November 2026. https://developers.google.com/earth-engine/datasets/catalog/COPERNICUS_S2_HARMONIZED

Google Earth Engine. (2026c). Harmonized Sentinel-2 MSI Level-2A surface reflectance. Earth Engine Data Catalog. Accessed 2 November 2026. https://developers.google.com/earth-engine/datasets/catalog/COPERNICUS_S2_SR_HARMONIZED

Google Earth Engine. (2026d). Sentinel-2 Cloud Probability. Earth Engine Data Catalog. Accessed 2 November 2026. https://developers.google.com/earth-engine/datasets/catalog/COPERNICUS_S2_CLOUD_PROBABILITY

Gorelick, N., Hancher, M., Dixon, M., Ilyushchenko, S., Thau, D., & Moore, R. (2017). Google Earth Engine: Planetary-scale geospatial analysis for everyone. Remote Sensing of Environment, 202, 18–27. https://doi.org/10.1016/j.rse.2017.06.031

Harper, K. A., Macdonald, S. E., Burton, P. J., Chen, J., Brosofske, K. D., Saunders, S. C., Euskirchen, E. S., Roberts, D., Jaiteh, M. S., & Esseen, P.-A. (2005). Edge influence on forest structure and composition in fragmented landscapes. Conservation Biology, 19(3), 768–782. https://doi.org/10.1111/j.1523-1739.2005.00045.x

Hausermann, H., Ferring, D., Atosona, B., Mentz, G., Amankwah, R., Chang, A., Hartfield, K., Effah, E., Asuamah, G. Y., Mansell, C., & Sastri, N. (2018). Land-grabbing, land-use transformation and social differentiation: Deconstructing “small-scale” in Ghana’s recent gold rush. World Development, 108, 103–114. https://doi.org/10.1016/j.worlddev.2018.03.014

Hilson, G., & Nyame, F. (2006). Gold mining in Ghana's forest reserves: A report on the current debate. Area, 38(2), 175–185. https://doi.org/10.1111/j.1475-4762.2006.00670.x

Ministry of Environment, Science and Technology. (2025). Minister initiates legal overhaul, seeks revocation of L.I. 2462 to curb illegal mining. Press release, 29 August 2025. https://www.mincom.gov.gh/wp-content/uploads/2025/08/Press-Release-Request-to-Revoke-LI-2462.pdf

Nunoo, S., Manu, J., Owusu-Akyaw, F. K. B., & Nyame, F. K. (2022). Impact of artisanal small-scale (gold and diamond) mining activities on the Offin, Oda and Pra rivers in Southern Ghana, West Africa: A scientific response to public concern. Heliyon, 8(12), e12323. https://doi.org/10.1016/j.heliyon.2022.e12323

Nyamekye, C., Ghansah, B., Agyapong, E., & Kwofie, S. (2021). Mapping changes in artisanal and small-scale mining (ASM) landscape using machine and deep learning algorithms: A proxy evaluation of the 2017 ban on ASM in Ghana. Environmental Challenges, 3, 100053. https://doi.org/10.1016/j.envc.2021.100053

Olofsson, P., Foody, G. M., Herold, M., Stehman, S. V., Woodcock, C. E., & Wulder, M. A. (2014). Good practices for estimating area and assessing accuracy of land change. Remote Sensing of Environment, 148, 42–57. https://doi.org/10.1016/j.rse.2014.02.015

Olofsson, P., Foody, G. M., Stehman, S. V., & Woodcock, C. E. (2013). Making better use of accuracy data in land change studies: Estimating accuracy and area and quantifying uncertainty using stratified estimation. Remote Sensing of Environment, 129, 122–131. https://doi.org/10.1016/j.rse.2012.10.031

Republic of Ghana. (2022). Environmental Protection (Mining in Forest Reserves) Regulations, 2022, L.I. 2462. https://ghalii.org/akn/gh/act/li/2022/2462/eng%402022-07-27

Republic of Ghana. (2025). Environmental Protection (Mining in Forest Reserves) (Amendment) Regulations, 2025, L.I. 2501. https://www.judy.legal/legislation/akn/gh/act/li/2025/2501

Schueler, V., Kuemmerle, T., & Schröder, H. (2011). Impacts of surface gold mining on land use systems in Western Ghana. Ambio, 40, 528–539. https://doi.org/10.1007/s13280-011-0141-9

Snapir, B., Simms, D. M., & Waine, T. W. (2017). Mapping the expansion of galamsey gold mines in the cocoa growing area of Ghana using optical remote sensing. International Journal of Applied Earth Observation and Geoinformation, 58, 225–233. https://doi.org/10.1016/j.jag.2017.02.009

Stehman, S. V. (2014). Estimating area and map accuracy for stratified random sampling when the strata are different from the map classes. International Journal of Remote Sensing, 35(13), 4923–4939. https://doi.org/10.1080/01431161.2014.930207

Tsai, Y.-H., Stow, D. A., López-Carr, D., Weeks, J. R., Clarke, K. C., & Mensah, F. (2019). Monitoring forest cover change within different reserve types in southern Ghana. Environmental Monitoring and Assessment, 191, 281. https://doi.org/10.1007/s10661-019-7450-z

UNEP-WCMC and IUCN. (2026). World Database on Protected Areas polygons. Protected Planet, accessed through Google Earth Engine. Accessed 2 November 2026. https://developers.google.com/earth-engine/datasets/catalog/WCMC_WDPA_current_polygons

Wanyama, D., Wimberly, M. C., & Mensah, F. (2023). Patterns and drivers of disturbance in tropical forest reserves of southern Ghana. Environmental Research Letters, 18(6), 064022. https://doi.org/10.1088/1748-9326/acd399

WHO. (2016). Environmental and occupational health hazards associated with artisanal and small-scale gold mining. World Health Organization, Geneva. https://www.who.int/publications/i/item/9789241510271

WHO. (2024). Mercury. Fact sheet, 24 October 2024. World Health Organization. https://www.who.int/news-room/fact-sheets/detail/mercury-and-health

Wimberly, M. C., Dwomoh, F. K., Numata, I., Mensah, F., Amoako, J., Nekorchuk, D. M., & McMahon, A. (2022). Historical trends of degradation, loss, and recovery in the tropical forest reserves of Ghana. International Journal of Digital Earth, 15(1), 30–51. https://doi.org/10.1080/17538947.2021.2012533

Abugre, S., Asigbaase, M., Kumi, S., Nkoah, G., & Asare, A. (2025). Forest landscape degradation, carbon loss and ecological consequences of illegal gold mining in Ghana. *Discover Forests, 1*, Article 20. https://doi.org/10.1007/s44415-025-00020-5

Barenblitt, A., Payton, A., Lagomasino, D., Fatoyinbo, L., Asare, K., Aidoo, K., Pigott, H., Som, C. K., Smeets, L., Seidu, O., & Wood, D. (2021). The large footprint of small-scale artisanal gold mining in Ghana. *Science of the Total Environment, 781*, Article 146644. https://doi.org/10.1016/j.scitotenv.2021.146644

Barend, T. A. (2026). *The ecological impacts of un-protecting forests: The case of gold mining in Ghana* [Master's thesis, University of San Francisco]. USF Scholarship Repository. https://repository.usfca.edu/thes/1646/

Coalition Against Galamsey–Ghana, A Rocha Ghana, Kasa Initiative Ghana, Eco-Conscious Citizens, BRACE, Nature and Development Foundation, WACAM, OXFAM, Christian Council of Ghana, Taylor Crabbe, Client Earth, Civic Response, Ghana Institute of Foresters, Ghana Environmental Advocacy Group, General Transport, Petroleum and Chemical Workers' Union of TUC (Ghana), Peasant Farmers Association, & SDG Civil Society Platform Ghana. (2025, December 18). *Commendations to government for revoking L.I. 2462; time to restore and enhance forest management and services to Ghanaians* [Joint press statement]. https://ghana.arocha.org/wp-content/uploads/sites/42/2025/12/PRESS-STATEMENT-LI2462-DEC-2025.pdf

Dong, L., Tang, X., Mensah, F., Abubakari, B. A., Bratley, K. H., Olofsson, P., & Woodcock, C. E. (2025). Near real-time monitoring reveals extensive recent forest disturbance in Ghana's protected areas. *Science of Remote Sensing, 12*, Article 100299. https://doi.org/10.1016/j.srs.2025.100299

Food and Agriculture Organization of the United Nations. (2025, October 21). *Global deforestation slows, but forests remain under pressure, FAO report shows*. https://www.fao.org/newsroom/detail/global-deforestation-slows--but-forests-remain-under-pressure--fao-report-shows/en

Forkuor, G., Ullmann, T., & Griesbeck, M. (2020). Mapping and monitoring small-scale mining activities in Ghana using Sentinel-1 time series (2015–2019). *Remote Sensing, 12*(6), Article 911. https://doi.org/10.3390/rs12060911

Hajjar, R. (2015). Advancing small-scale forestry under FLEGT and REDD in Ghana. *Forest Policy and Economics, 58*, 12–20. https://doi.org/10.1016/j.forpol.2014.09.014

Mensah-Odum, N., Sarfo-Mensah, P., & Fredua-Antoh, E. (2025). Legal and regulatory evidence on mining in Ghana forest reserves: A qualitative perspective on the Atewa Range Forest Reserve. *European Journal of Applied Sciences, 13*(3), 421–434. https://doi.org/10.14738/aivp.1303.18806

Olofsson, P., Foody, G. M., Herold, M., Stehman, S. V., Woodcock, C. E., & Wulder, M. A. (2014). Good practices for estimating area and assessing accuracy of land change. *Remote Sensing of Environment, 148*, 42–57. https://doi.org/10.1016/j.rse.2014.02.015

Olofsson, P., Foody, G. M., Stehman, S. V., & Woodcock, C. E. (2013). Making better use of accuracy data in land change studies: Estimating accuracy and area and quantifying uncertainty using stratified estimation. *Remote Sensing of Environment, 129*, 122–131. https://doi.org/10.1016/j.rse.2012.10.031

Pillay, R., Venter, M., Aragon-Osejo, J., González-del-Pliego, P., Hansen, A. J., Watson, J. E. M., & Venter, O. (2022). Tropical forests are home to over half of the world's vertebrate species. *Frontiers in Ecology and the Environment, 20*(1), 10–15. https://doi.org/10.1002/fee.2420

Schueler, V., Kuemmerle, T., & Schröder, H. (2011). Impacts of surface gold mining on land use systems in Western Ghana. *Ambio, 40*(5), 528–539. https://doi.org/10.1007/s13280-011-0141-9

Shrestha, U. B., Chaudhary, T., & Shrestha, S. (2025). Major forest biodiversity and ecosystem goods and services. In P. Saikia, A. Kumar, M. L. Khan, & X. Lei (Eds.), *Forests for inclusive and sustainable economic growth* (pp. 269–280). Elsevier. https://doi.org/10.1016/B978-0-443-31406-3.00020-5

Upadhyay, P., & Singh, T. S. (2024). The importance of conserving existing forest areas and protecting biodiversity in addressing climate change issues. In H. Singh (Ed.), *Forests and climate change: Biological perspectives on impact, adaptation, and mitigation strategies* (pp. 605–623). Springer. https://doi.org/10.1007/978-981-97-3905-9_29

Supplementary Table S1 Annual land-cover areas by reserve (ha)

a Upper Wassaw

Land-cover class	2016	2020	2025
Forest / Tree Cover	12,956.67	12,400.63	11,956.01
Shrub / Grassland	65.87	57.86	236.42
Cropland	80.77	115.31	312.91
Built-up	255.55	730.20	831.21
Bare / Disturbed Land	127.87	159.81	158.99
Water	97.87	103.86	91.85
Flooded Vegetation	15.69	34.11	14.15
Eligible frame	13,600.29	13,601.78	13,601.54

Source: Authors' calculations.

b Oda River

Land-cover class	2016	2020	2025
Forest / Tree Cover	16,333.58	16,795.78	15,521.27
Shrub / Grassland	9.36	0.33	241.03
Cropland	1.61	2.02	309.99
Built-up	2.66	8.75	403.20
Bare / Disturbed Land	6.60	4.20	277.43
Water	458.08	8.26	64.02
Flooded Vegetation	5.11	0.84	3.24
Eligible frame	16,817.00	16,820.18	16,820.18

Source: Authors' calculations.

c Apamprama

Land-cover class	2016	2020	2025
Forest / Tree Cover	3,692.75	3,620.11	2,635.52

Shrub / Grassland	1.01	1.56	251.85
Cropland	0.57	7.21	364.33
Built-up	0.26	24.05	179.78
Bare / Disturbed Land	7.42	28.60	226.50
Water	2.82	24.00	44.28
Flooded Vegetation	2.65	1.95	5.22
Eligible frame	3,707.48	3,707.48	3,707.48

860 Source: Authors' calculations.